Quantum Graphs and Applications

Marcos G. E. da Luz[§]

Verão Quântico 2019

Feb 17-22, Ubu-Anchieta, ES, Brazil

[§]Universidade Federal do Paraná-UFPR
Curitiba-PR, Brazil

Oultine

- Path integrals and Green's functions (a brief review)
- Graph structures
- Semiclassical-like approximation (made exact)
- Quantum qraphs (through Green's functions):

  “a sum over paths” approach
- Examples
- Final conclusions

A) Time-dependent Propagator

• In quantum mechanics (with $|\Psi(t_i)\rangle$ known)

$$\hat{H}(t_f)|\Psi(t_f)\rangle \;=\; i\hbar\frac{\partial}{\partial t_f}|\Psi(t_f)\rangle.$$

Defining ($\hat{\mathcal{U}}(t,t)=\mathbf{1}$)

$$|\Psi(t_f)\rangle \;=\; \hat{\mathcal{U}}(t_f,t_i)|\Psi(t_i)\rangle,$$

then

$$\hat{H}(t_f)\hat{\mathcal{U}}(t_f,t_i) \;=\; i\hbar\frac{\partial}{\partial t_f}\hat{\mathcal{U}}(t_f,t_i).$$

For $\hat{\mathcal{T}}$ being the time ordering operator (identity operator) if $[\hat{H}(t''),\hat{H}(t')]\neq 0$ ($[\hat{H}(t''),\hat{H}(t')]=0$), with $t''\neq t'$, formally

$$\hat{\mathcal{U}}(t_f,t_i) \;=\; \hat{\mathcal{T}}\exp\left[-\frac{i}{\hbar}\int_{t_i}^{t_f}dt\,\hat{H}(t)\right].$$

• In non-relativistic quantum mechanics we are most interested in causal processes, namely, $t_f\geq t_i$. In this way, one can define the time-dependent propagator in the representation μ—ν as [for $\theta(\cdot)$ the usual step function, with $\partial\theta(\cdot)/\partial\,\cdot=\delta(\cdot)$ Dirac's delta function]

$$\begin{aligned} K(\mu_f,t_f;\nu_i,t_i) \;&=\; \langle\mu_f|\hat{K}(t_f,t_i)|\nu_i\rangle,\\ \hat{K}(t_f,t_i) \;&=\; \theta(t_f-t_i)\hat{\mathcal{U}}(t_f,t_i).\end{aligned}$$

By choosing: $\mu = \nu = \mathbf{r}$, $\mu = \nu = \mathbf{p}$, $\mu = \nu = \mathbf{r} + i\mathbf{p}$, and $\mu = \mathbf{p}$, $\nu = \mathbf{r}$, we have, respectively, configuration, momenta, coherent state, and Kirkwood, representations.

• From the blue equations we get

$$\left[\hat{H}(t_f) - i\hbar\frac{\partial}{\partial t_f}\right]\hat{K}(t_f, t_i) \;=\; -i\hbar\,\delta(t_f - t_i)\,\mathbf{1},$$

which in the configuration representation reads

$$\left[H(\mathbf{r}_f; t_f) - i\hbar\frac{\partial}{\partial t_f}\right]K(\mathbf{r}_f, t_f; \mathbf{r}_i, t_i) \;=\; -i\hbar\,\delta(t_f - t_i)\,\delta(\mathbf{r}_f - \mathbf{r}_i).$$

Surely, the above is a Green's function type of equation, hence

$$\langle \mathbf{r}_f|\Psi(t_f)\rangle \;=\; \int d\mathbf{r}_i\, K(\mathbf{r}_f, t_f; \mathbf{r}_i, t_i)\,\langle \mathbf{r}_i|\Psi(t_i)\rangle.$$

• Suppose (at least in principle) an appropriate time-dependent orthonormal basis $\{|\phi_n(t)\rangle, |\varphi_\sigma(t)\rangle\}$ for the problem. Then, from $\sum_n |\phi_n(t)\rangle\langle\phi_n(t)| + \int d\sigma\, |\varphi_\sigma(t)\rangle\langle\varphi_\sigma(t)| = \mathbf{1}$ (valid for any time) and the definition of K, it follows that

$$\begin{aligned} K(\mathbf{r}_f, t_f; \mathbf{r}_i, t_i) \;=\; & \sum_n \phi_n(\mathbf{r}_f, t_f)\,\phi_n^*(\mathbf{r}_i, t_i) \\ & + \int d\sigma\, \varphi_\sigma(\mathbf{r}_f, t_f)\,\varphi_\sigma^*(\mathbf{r}_i, t_i). \end{aligned}$$

B) Energy-dependent Green's function

• Suppose $\hat{H} \neq \hat{H}(t)$ and let us set $t_f = t$ and $t_i = t_0$. One can define the energy-dependent Green's function as

$$\hat{G}(E) \;=\; \frac{1}{i\hbar}\int_{-\infty}^{+\infty} d\tau \; \exp[\frac{i}{\hbar}E\,\tau]\hat{K}(\tau).$$

• Considering the magenta equation for $\hat{K}$ and the above expression for $\hat{G}$, we find (assuming $\mathrm{Im}[E] = \varepsilon$ and $\varepsilon \to 0^+$)

$$(E - \hat{H})\,\hat{G}(E) = \mathbf{1}, \quad \text{or} \quad \hat{G}(E) \;=\; (E - \hat{H})^{-1}.$$

Therefore, $\hat{G}(E)$ is the resolvent of the system Hamiltonian.

• Inserting a (time-independent) basis, for which $\Sigma_n\,|\phi_n\rangle\langle\phi_n| + \int d\sigma\,|\varphi_\sigma\rangle\langle\varphi_\sigma| \;=\; \mathbf{1}$, into $G(\mathbf{r}_f, \mathbf{r}_i; E) \;=\; \langle \mathbf{r}_f|(E - \hat{H})^{-1}|\mathbf{r}_i\rangle$ $(E = \hbar^2 k^2/(2m))$,

$$G(\mathbf{r}_f, \mathbf{r}_i; k) \;=\; \frac{2m}{\hbar^2}\sum_n \frac{\phi_n(\mathbf{r}_f)\,\phi_n^*(\mathbf{r}_i)}{(k^2 - k_n^2)} + \frac{2m}{\hbar^2}\int_0^{+\infty} d\sigma\,\frac{\varphi_\sigma(\mathbf{r}_f)\,\varphi_\sigma^*(\mathbf{r}_i)}{(k^2 - \sigma^2)}.$$

The poles of G result from the discrete and the G branch cuts come from the continuous states.

C) Feynman's path integrals

• In a brilliant insight (as typical!) [*Physikaalische Z. der Sowjetunion* **3**, 64 (1933)], Dirac mentioned that infinitesimal quantum transitions can be described by the classical Lagrangian. In the simpler case ($\hat{H} = \hat{T} + \hat{V}$) for order $\mathcal{O}(\delta t^1)$

$$\begin{aligned}
K(\mathbf{r}'', \mathbf{r}'; \delta t) &= \langle \mathbf{r}'' | \exp[-\frac{i}{\hbar}(\hat{T} + \hat{V})\delta t] | \mathbf{r}' \rangle \\
&\approx \langle \mathbf{r}'' | \exp[-\frac{i}{\hbar}\hat{V}\delta t] \exp[-\frac{i}{\hbar}\hat{T}\delta t] | \mathbf{r}' \rangle \\
&= \int d\mathbf{r}\, d\mathbf{p}\, \langle \mathbf{r}'' | \exp[-\frac{i}{\hbar}\hat{V}\delta t] | \mathbf{r} \rangle \\
&\quad \times \langle \mathbf{r} | \exp[-\frac{i}{\hbar}\hat{T}\delta t] | \mathbf{p} \rangle \langle \mathbf{p} | \mathbf{r}' \rangle \\
&= \int d\mathbf{p}\, \exp[-\frac{i}{\hbar}(T(\mathbf{p}) + V(\mathbf{r}))\delta t] \\
&\quad \times \langle \mathbf{r}'' | \mathbf{p} \rangle \langle \mathbf{p} | \mathbf{r}' \rangle \\
&= \int d\mathbf{p}\, \exp[-\frac{i}{\hbar}(T(\mathbf{p}) + V(\mathbf{r}''))\delta t] \\
&\quad \times \frac{1}{(2\pi\hbar)^{D/2}} \exp[+\frac{i}{\hbar}\mathbf{p} \cdot (\mathbf{r}'' - \mathbf{r}')]
\end{aligned}$$

Recalling that $L = \mathbf{p} \cdot \dot{\mathbf{r}} - H$, $S = \int_{t'}^{t''} dt\, L(\mathbf{r}, \dot{\mathbf{r}}) \approx L(\mathbf{r}'', \dot{\mathbf{r}}')\, \delta t$ (with $t'' - t' = \delta t$) and assuming quadratic kinetic energy, $T(\mathbf{p}) = \mathbf{p}^2/(2m)$, the above integral is a simple Gaussian, so

$$\begin{aligned}
K(\mathbf{r}'', \mathbf{r}'; \delta t) &\approx \left(\frac{m}{2\pi i\hbar\delta t}\right)^{D/2} \exp[\frac{i}{\hbar}\delta t\, L(\mathbf{r}'', \dot{\mathbf{r}}'')] \\
&\approx \left(\frac{m}{2\pi i\hbar\delta t}\right)^{D/2} \exp[\frac{i}{\hbar}S(t'', t')]
\end{aligned}$$

• Feynman in an even brighter insight [Rev. Mod. Phys. **58**, 449 (1986)] has used such idea (for some historical account, see S. Schweber, Rev. Mod. Phys. **58**, 449 (1986)]) calculating a finite time quantum transition as ($t_f = t_{N+1}$, $t_i = t_0$; $\mathbf{r}_f = \mathbf{r}_{N+1}$, $\mathbf{r}_i = \mathbf{r}_0$;)

$$\begin{aligned} K(\mathbf{r}_f, t_f; \mathbf{r}_i; t_i) &= \langle \mathbf{r}_f | \hat{\mathcal{U}}(t_f, t_i) | \mathbf{r}_i \rangle \\ &= \langle \mathbf{r}_f | \Pi_{n=1}^{n=N+1} \hat{\mathcal{U}}(t_n, t_{n-1}) | \mathbf{r}_i \rangle \\ &= \left[\Pi_{j=1}^{j=N} \int d\mathbf{r}_j \right] \Pi_{n=1}^{n=N+1} \langle \mathbf{r}_n | \hat{\mathcal{U}}(t_n, t_{n-1}) | \mathbf{r}_{n-1} \rangle, \end{aligned}$$

which in the limits: $(t_n - t_{n-1})$ going to zero and N going to infinity; has the final expression in a somehow formal notation ($P \equiv (\mathbf{r}, t)$)

$$K(\mathbf{r}_f, t_f; \mathbf{r}_i, t_i) = \int_{P_i}^{P_f} D[\mathbf{r}(\tau)] \exp[\frac{i}{\hbar} S(\mathbf{r}(\tau))] \ (*).$$

• This formalism for the quantum mechanics has promoted tremendous progress in many areas, allowing a different view on a broad range of distinct phenomena. Certainly, this one and the whole series of path integral conferences are good examples of the great success of such approach to physics.

• Much has be done using $(*)$, as seen from sources as

Semiclassical approximation and (just a bit) beyond

• In our previous $(*)$, basically $D[\mathbf{r}(\tau)]$ says we should consider *all imaginable* paths leaving from P' and getting to P'', calculate (given the potential V) the corresponding action S, and then finally to sum up all these contributions, so to obtain the quantum propagator. A formidable task indeed! Can we make things a little easier?

• Well, let us look at $\exp[\frac{i}{\hbar}S(\mathbf{r}(\tau))]$. This may be a rather oscillatory function, depending on the character of the different paths. So, we can expect many cancellations as we sum over $\mathbf{r}(\tau)$. But hopefully, a certain class of paths might end up contributing the most to K.

• In classical mechanics we know that $\delta S = 0$ is the condition to determine the system correct classical trajectories. So, the idea is then to write K *only* as a sum over the trajectories of the corresponding classical system. Doing properly the calculations (via stationary phase ideas), one gets the Van Vleck-Gutzwiller formula [J.H. Van Vleck, Proc. Nat. Acad. Sci. USA **14**, 178 (1928); M.C. Gutzwiller, J. Math. Phys. **8**, 1979 (1967)], or (χ the Morse index: # of conjugate points)

$$K_{sc} = \frac{1}{(2\pi i\hbar)^{D/2}} \sum_{cl} \sqrt{C_{cl}(P_f, P_i)}\, \exp[\frac{i}{\hbar} S_{cl}(P_f, P_i) - i\frac{\pi}{2}\chi_{cl}].$$

C_{cl} is associated to the density of trajectories.

• The energy-dependent Green function is just the Fourier transform of K (for time-independent problems). So, one could write K as the path integral expression, to perform an extra integration (over time) and finally to consider the stationary phase approach [see M.C. Gutzwiller, *Chaos in Classical and Quantum Mechanics* (Springer-Verlag, 1990)]. Thus

$$G_{sc}(E) = \frac{2\pi}{(2\pi i\hbar)^{(D+1)/2}} \sum_{cl} M_{cl} \exp[\frac{i}{\hbar} S_{cl}(\mathbf{r}_f, \mathbf{r}_i; E) - i\frac{\pi}{2}\eta_{cl}],$$

$$M_{cl} = \left[\frac{1}{|\dot{\mathbf{r}}_f||\dot{\mathbf{r}}_i|}(-1)^{D+1}\det(-\partial S^2/\partial \mathbf{r}_f\, \partial \mathbf{r}_i)|_{red}\right]^{1/2}.$$

Again M_{cl} is related to the density of the classical trajectories.

• Can one extend the above expression? The answer is a (considerably courageous!) yes simply proposing the *ansatz*

$$G_{gsc}(E) = \sum_{sp} W_{sp} \exp[\frac{i}{\hbar} S_{sp}(\mathbf{r}_f, \mathbf{r}_i; E)].$$

The sum is performed over a class of paths (let us call then "special paths"), with the amplitude W_{sp} weighting the contribution of each *sp* to the sum.

• The big questions are hence: (1) Are there systems for which the above expression is a good approximation; (2) In case there exist, is it possible to identify these "special paths"? In general I have no clue, but for graphs we can say yes.

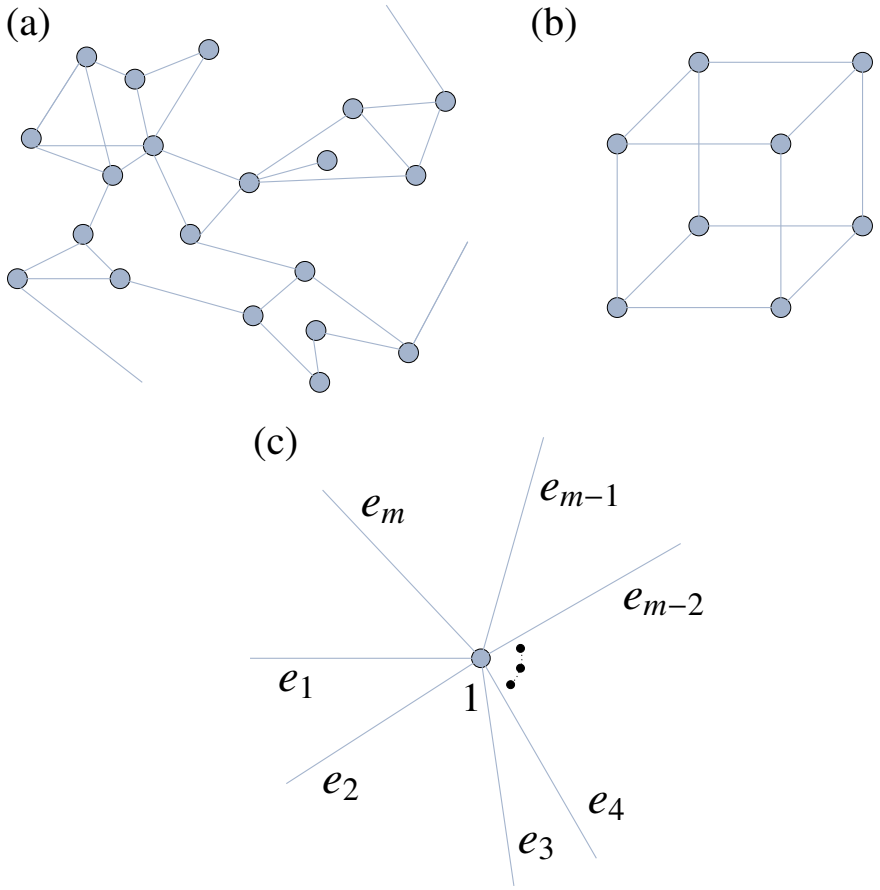

Figure 1: Examples of (a) open and (b) closed quantum graphs. (c) A open star graph with a single vertex $V(\Gamma = \{1\}$ connected to $E(\Gamma) = \{e_1, \ldots, e_m\}$ leads.

A *quantum graph* is a metric graph structure $\Gamma(V, E)$, on which we can define a differential operator H (usually the Schrödinger Hamiltonian) together with proper vertices boundary conditions.

A schematic representation of quantum graphs is depicted in Figure 1.

The total wave function Ψ is a vector with m components, written as

$$\Psi = \begin{pmatrix} \psi_{e_1}(x_{e_1}) \\ \psi_{e_2}(x_{e_2}) \\ \vdots \\ \psi_{e_m}(x_{e_m}) \end{pmatrix}. \tag{1}$$

The Hamiltonian operator on $E(\Gamma)$ consists of the following unidimensional differential operators defined on each edge e_s (the dressed case)

$$H_{e_s}(x_{e_s}) = -\frac{\hbar^2}{2\mu}\frac{d^2}{dx_{e_s}^2} + V_{e_s}(x_{e_s}). \tag{2}$$

Here, $V_{e_s}(x_{e_s})$ is the potential (usually assumed to be non-negative and smooth) in the interval $0 < x_{e_s} < \ell_{e_s}$. It is usual to have for any e_s that $V_{e_s} = 0$. Then, the component $\psi_{e_s}(x_{e_s})$ of the full Ψ is the solution of ($k = \sqrt{2\mu E}/\hbar$)

$$-\frac{d^2\psi_{e_s}}{dx_{e_s}^2} = k^2\psi_{e_s}(x_{e_s})$$

$$\psi_{e_s}(x_{e_s}) = c_{+,e_s}\,\exp[+i\,k\,x_{e_s}] + c_{-,e_s}\,\exp[-i\,k\,x_{e_s}].$$

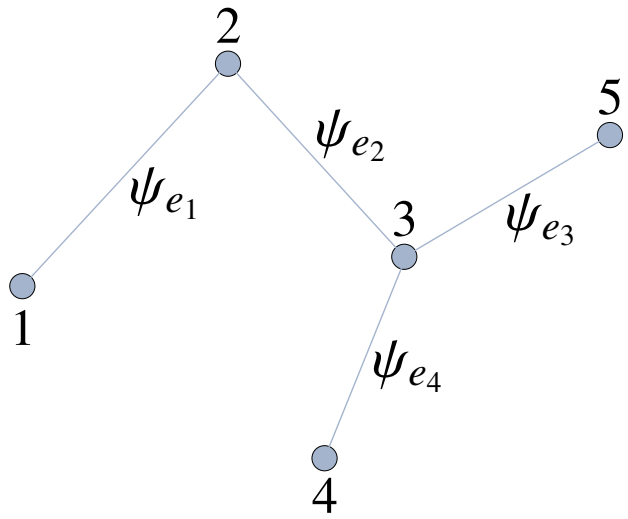

Figure 2: A quantum graph with $V(\Gamma) = \{1, 2, 3, 4, 5\}$ and $E(\Gamma) = \{\{1, 2\}, \{2, 3\}, \{3, 4\}, \{3, 5\}\}$ and the indication of the ψ_{e_s} components of Ψ in each one of the Γ edges. The wave functions must be matched through the boundary condition at each vertex $i \in V(\Gamma)$. Specifically: at $i = 1$: ψ_{e_1}; at $i = 2$: ψ_{e_1}, ψ_{e_2}; at $i = 3$: $\psi_{e_2}, \psi_{e_3}, \psi_{e_4}$; at $i = 4$: ψ_{e_4}; at $i = 5$: ψ_{e_3}.

All these wave functions must satisfy appropriate boundary conditions at the vertices.

Technically, the match of the boundary conditions in each vertex is the most cumbersome step in obtaining the final full Ψ (in Figure 2 we illustrate which components must be matched in which vertices for a particular example).

• In an undressed graph edges e_s can be viewed as free 1D spatial directions of length ℓ_{e_s}.

• The vertices are point structures (0D), whose action is to impose the proper boundary conditions on the ψ's.

• In the usual 1D quantum mechanics, arbitrary zero-range potentials, also known as point interactions, have exactly such effect. A textbook example is the Dirac delta-function potential.

• Hence, to describe the quantum dynamics along a graph we can take the j's as arbitrary zero-range interactions:

(a) The j's become point scatterers, which are completely characterized by their reflections and transmission amplitudes.
(b) General point interactions are very diverse in their scattering properties.

• We define for each vertex j a matrix $\mathcal{S}_j$ of elements $\mathcal{S}_j^{(s,s)}(k) = r_j^{(s)}(k)$ and $\mathcal{S}_j^{(s,r)}(k) = t_j^{(s,r)}(k)$ (we label edges e_{js} and e_{jr} simply as s and r):

(i) $t_j^{(s,r)}(k)$ is the quantum amplitude for a plane wave, of wave number k, incoming from the edge r towards the vertex j to be transmitted to the edge s outgoing from j.

(ii) $r_j^{(s)}(k)$ is the quantum amplitude for a plane wave, of wave number k, incoming from the edge s towards the vertex j to be reflected to the edge s outgoing from j.

• The required conditions for probability flux conservation along the whole graph demands that $\mathcal{S}(k)\mathcal{S}^\dagger(k) = \mathcal{S}^\dagger(k)\mathcal{S}(k) = \mathbf{1}$ and $\mathcal{S}(k) = \mathcal{S}^\dagger(-k)$ at each vertex.

• The *exact* Green's function for an arbitrary finite 1D array of potentials of compact support[1] has exactly the form of a Generalized Semiclassical Expression.

• For these general array of potentials, the exact Green's function for a fixed energy E (and end points x_i and x_f) is given by

$$G(E) = \frac{m}{i\hbar^2 k} \sum_{sp} W_{sp} \exp\left[\frac{i}{\hbar} S_{sp}(x_f, x_i; k)\right].$$

• The above sum is performed over all scattering paths (sp) starting in x_i and ending in x_f. A 'scattering path' represents a trajectory in which the particle leaves from x_i, suffers multiple scattering, and finally arrives at x_f.

---

[1] $V_n(x)$ is said to have compact support in the interval $\mathcal{I}_n \equiv \{x \,|\, a_n < x < b_n\}$ if $V_n(x)$ identically vanishes for $x \notin \mathcal{I}_n$. An arbitrary array of N potentials of compact support is given by $V(x) = \sum_{n=1}^{N} V_n(x)$, for all $\mathcal{I}_n$'s disjoint.

• $S_{sp} = k L_{sp}$ is the classical-like action, with L_{sp} the trajectory length. W_{sp} is the sp weight, constructed as the following: each time the particle hits a potential V_n, it can be reflected or transmitted by it. In the first case, W_{sp} gets a factor r_n and in the second, W_{sp} gets a factor t_n. The total W_{sp} is then the product of all quantum coefficients r_n's and t_n's acquired along the sp.

• The extension to quantum graphs is natural. The two main ingredients necessary in the derivations, namely, unidimensionality and localized potentials, are by construction present in graphs.

(i) First, since the quantum evolution takes place along the graph edges, regardless the graph topology, the dynamics is essentially 1D.

(ii) Second, the potentials (scatters) are the vertices, which can be treated as point interactions, a particular class of compact support potentials.

EXAMPLE 1

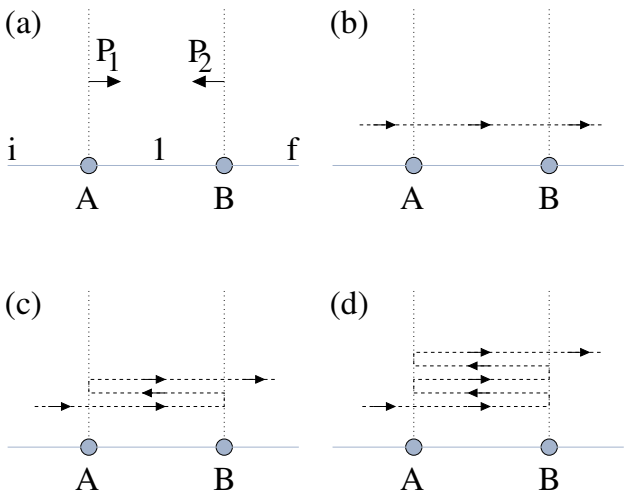

Figure 3: A simple graph with two vertices, A and B, a finite edge labeled 1 (of length ℓ_1), and left, i, and right, f, leads. (a) The starting positions of two families, P_1 and P_2, of sp. (b)-(d) Schematic examples of individual sp.

This open graph has two vertices, A and B, one finite edge (of length ℓ_1) 1, and two semi-infinite edges (leads), i and f. For $0 \leq x_i < +\infty$ ($x_i = 0$ at A) in i and $0 \leq x_f < +\infty$ ($x_f = 0$ at B) in f, $G_{fi}(x_f, x_i; k)$ describes the transmission across the full structure, i.e., from the left to the right leads.

• Notation

(a) $r_j^{(s)}$ and $t_j^{(s,r)}$ are the reflection and transmission amplitudes for the vertex j.

(b) P_l represents the contribution from an entire infinite family l of sp, so that $G = m/(i\hbar^2 k) \sum_l P_l$.

• To obtain G we need to sum up all the possible sp for a particle starting at x_i, in i, going through multiple reflections between the vertices A and B, and ending up at x_f, in f.

• In Fig. 3 (b)–(d) it is depicted three sp's.

• The scattering path in Fig. 3 (b) represents the 'direct' propagation from x_i to x_f. For it, the sp of Fig. 3 (b) contributes to G with

$W_{sp} = t_A^{(1,i)}\, t_B^{(f,1)}$ and

$L_{sp} = (x_f + x_i) + \ell_1$ (the length of this sp).

• Following the same type of analysis, we have:

$$\text{(c) } W_{sp} = r_A^{(1)}\, r_B^{(1)}\, t_A^{(1,i)}\, t_B^{(f,1)},$$
$$L_{sp} = (x_f + x_i) + 3\ell_1;$$
$$\text{(d) } W_{sp} = (r_A^{(1)})^2\, (r_B^{(1)})^2\, t_A^{(1,i)}\, t_B^{(f,1)},$$
$$L_{sp} = (x_f + x_i) + 5\ell_1.$$

• The full Green's function is written as a sum over all the existing terms of the above form, or

$$G_{fi} = \frac{m}{i\hbar^2 k} \exp[ikx_i]\, t_A^{(1,i)} \times \Big(\sum_{n=0}^{\infty} [r_A^{(1)}]^n\, [r_B^{(1)}]^n\, \exp[ik(2n+1)\ell_1] \Big) \times t_B^{(f,1)}\, \exp[ikx_f].$$

• The above is in fact a convergent geometric series since $|r_j^{(s)}|^2 \leq 1$ and $|t_j^{(s,r)}|^2 \leq 1$.

• So, the Green's function reads

$$G_{fi}(x_f, x_i; k) = \frac{m}{i\hbar^2 k} T_{fi} \exp[ik(x_f + x_i + \ell_1)],$$

with

$$T_{fi} = \frac{t_A^{(1,i)} t_B^{(f,1)}}{1 - r_A^{(1)} r_B^{(1)} \exp[2ik\ell_1]}.$$

• Note that Eq. T_{fi} can be recognized as the transmission amplitude for the whole system.

• This illustrates the fact that by properly regrouping several vertices, they can be treated as a 'single' vertex, effectively contributing with overall reflection and transmission amplitudes to G.

• Such a feature strongly simplifies the calculation of the Green's function for more complicated systems.

• For our example, to identify all the infinite possible sp is relatively direct. But when the number of vertices and edges increases, this can become a very tedious and cumbersome enterprise. Fortunately, the task can be accomplished by means of a simple diagrammatic scheme, separating the sp into families.

• To illustrate it, consider again G_{fi} for the graph of Fig. 3. For any sp, necessarily at the beginning the particle leaves x_i, goes to A, and then is transmitted through A. Once tunneling to $x_1 = 0^+$ (always with positive velocity), there are infinite possibilities to follow (some displayed in Fig. 3 (b)–(d)).

• So, schematically we represent all the trajectories headed to the right, departing from $x_1 = 0^+$, as the family P_1, Fig. 3 (a).

• Now, a sp in P_1 initiates traveling from A to B. Then, in B it may either cross the vertex B, finally arriving at the final point x_f, or be reflected from B, reversing its movement direction (at $x_1 = \ell_1^-$). For this latter situation, all the subsequent trajectories from $x_1 = \ell_1^-$ can be represented as the family P_2, Fig. 3 (a).

• But exactly the same reasoning shows that for any sp in P_2, the particle leaves B towards A, it is reflected from A, and then becomes one of the paths in P_1.

• Hence, the above prescription yields for the Green's function

$$G_{fi}(x_f, x_i; k) = \frac{m}{ik\hbar^2} \exp[ikx_i]\, t_A^{(1,i)}\, P_1,$$

where

$$P_1 = \exp[ik\ell_1] \begin{cases} r_B^{(1)}\, P_2 \\ t_B^{(f,1)} \exp[ikx_f], \end{cases}$$

and

$$P_2 = \exp[ik\ell_1]\, r_A^{(1)}\, P_1.$$

• '{' represents the possible splitting for the sp in the family P_1.

• The algebraic equation equivalent for P_1 is

$$P_1 = \exp[ik\ell_1]\Big(r_B^{(1)}\, P_2 + t_B^{(f,1)}\, \exp[ikx_f]\Big).$$

• Thus, solving for P_1 and P_2, one obtains

$$P_1 = \frac{t_B^{(f,1)}\, \exp[ik\ell_1]\, \exp[ikx_f]}{1 - r_A^{(1)}\, r_B^{(1)}\, \exp[2ik\ell_1]}.$$

• By direct substitution into the present G, we get the previous exact formula.

• In this way, the identification and summation of an infinite number of sp is reduced to the solution of a simple system of linear algebraic equations.

EXAMPLE 2

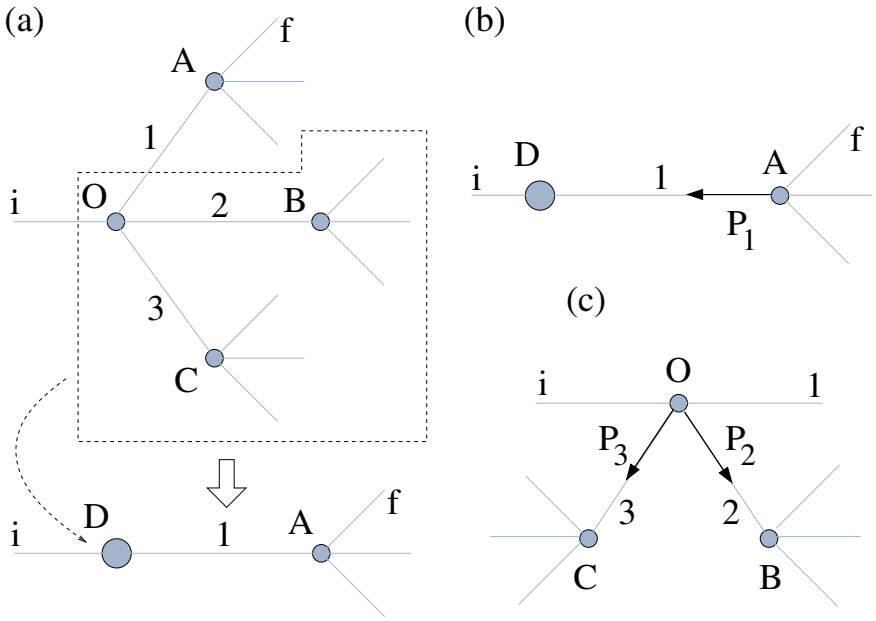

Figure 4: A tree-like quantum graph. (a) By regarding the whole region C—O—B (including the leads) as an 'unique' effective vertex D, the original graph is reduced as illustrated. (b) In the reduced graph, P_1 represents the family of trajectories which suffer multiple reflections between D and A, and finally tunnel the vertex A to the lead f. (c) The auxiliary graph (and the corresponding sp families) necessary to calculate $r_D^{(1)}$ and $t_D^{(i,1)}$.

• We can simplify the calculations for a large quantum graph by decomposing it in blocks, as done for the example shown in Fig. 4 (a).

• Suppose the Green's function for the initial position x_i in lead i and the end position x_f in lead f (Fig. 4 (a)).

• We then treat the whole block indicated in Fig. 4 (a) as a single vertex D. Any information about the inner structure of such region will be contained in the amplitudes $t_D^{(1,i)}$ and $r_D^{(1)}$. Thus, we reduce the original graph to the simpler one depicted in Fig. 4 (b).

• From Fig. 4 (b), we have that the Green's function can be written as

$$G_{fi}(x_f, x_i; k) = m/(i\hbar^2 k)\, T_{fi}\, \exp[ik(x_f + x_i)],$$

with

$$T_{fi} = t_D^{(1,i)} \exp[ik\ell_1]\left(r_A^{(1)} P_1 + t_A^{(f,1)}\right).$$

• Then, the infinite family of trajectories P_1 yields $P_1 = r_D^{(1)} \exp[2ik\ell_1]\big(r_A^{(1)} P_1 + t_A^{(f,1)}\big)$, or

$$P_1 = \frac{r_D^{(1)} t_A^{(f,1)} \exp[2ik\ell_1]}{1 - r_D^{(1)} r_A^{(1)} \exp[2ik\ell_1]}. \qquad (3)$$

• It remains to determine the coefficients $t_D^{(1,i)}$ and $r_D^{(1)}$. They follow from the auxiliary quantum graph of Fig. 4 (c).

• Recall that $t_D^{(1,i)}$ ($r_D^{(1)}$) represents the sp contribution for the particle to go from lead i (edge 1) to edge 1 through the region B—O—C. Inspecting Fig. 4 (c), we see that $t_D^{(1,i)} = t_O^{(1,i)} + t_O^{(3,i)} P_3 + t_O^{(2,i)} P_2$ and $r_D^{(1)} = r_O^{(1)} + t_O^{(3,1)} P_3 + t_O^{(2,1)} P_2$, where for the P's

$$\begin{cases} P_3 = r_C^{(3)} \exp[2ik\ell_3]\big(r_O^{(3)} P_3 + t_O^{(2,3)} P_2 + t_O^{(1,3)}\big) \\ P_2 = r_B^{(2)} \exp[2ik\ell_2]\big(r_O^{(2)} P_2 + t_O^{(3,2)} P_3 + t_O^{(1,2)}\big). \end{cases}$$

• The above is readily solved.

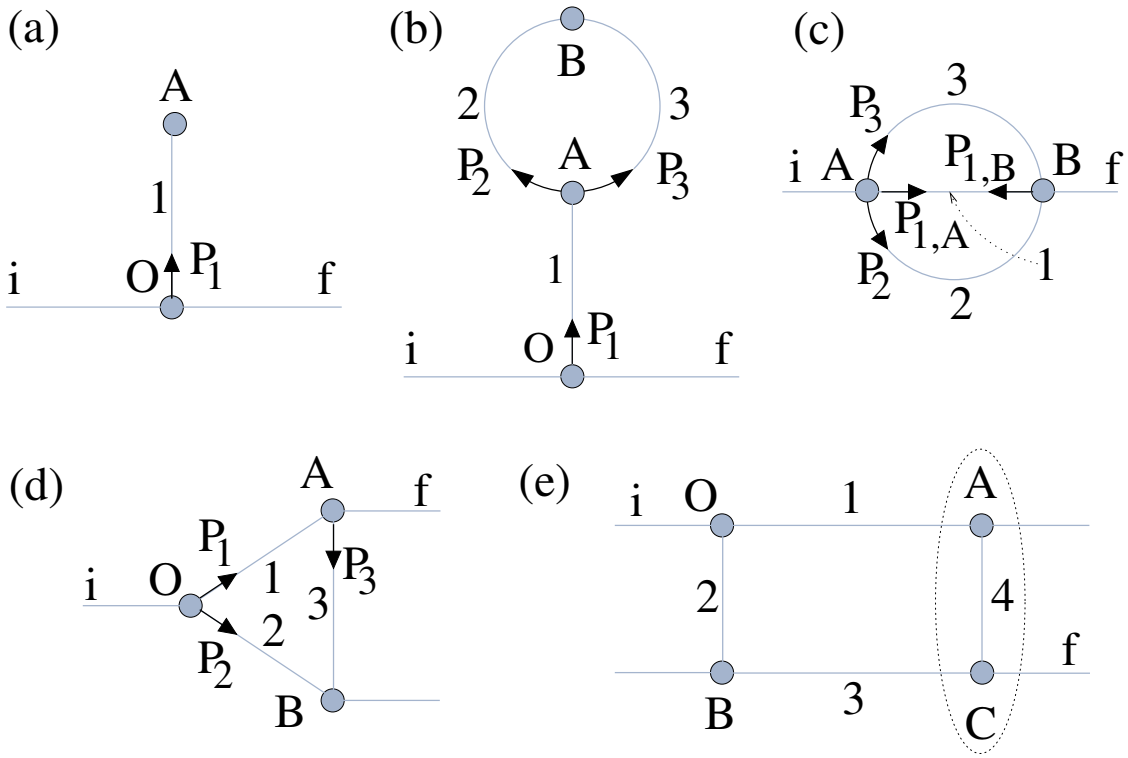

Figure 5: Several graphs whose G's can be obtained from the solutions of other topologies by eliminating, redefining or regrouping the vertices reflections and transmissions quantum amplitudes.

• The Green's function with x_i in lead i and x_f in lead f for the graph in Fig. 5 (a) is

$$G_{fi}(x_f, x_i; k) = \frac{m}{i\hbar^2 k} T_{fi} \exp[ik(x_f + x_i)],$$

$$T_{fi} = t_O^{(f,i)} + \frac{t_O^{(1,i)} r_A^{(1)} t_O^{(f,1)} \exp[2ik\ell_1]}{1 - r_O^{(1)} r_A^{(1)} \exp[2ik\ell_1]}.$$

• For both x_i and x_f ($0 < x_i, x_f < \ell_1$, $x_f > x_i$) in the edge 1, we get

$$\begin{aligned} G_{11}(x_f, x_i; k) = \frac{m}{i\hbar^2 k} & \frac{1}{\left(1 - r_O^{(1)} r_A^{(1)} \exp[2ik\ell_1]\right)} \\ & \times \left(\exp[-ikx_i] + r_O^{(1)} \exp[ikx_i]\right) \\ & \times \left(\exp[ikx_f] + r_A^{(1)} \exp[2ik\ell_1]\right. \\ & \left. \times \exp[-ikx_f]\right). \end{aligned}$$

• For open graphs, like that in Fig. 5 (a), depending on the characteristics of the vertices, the system may support bound states (a trivial textbook example is the usual δ-function potential in the line: if its strength γ is negative, the problem has exactly one bound state).

• In these cases, the eigenstates are calculated from the residues of $G(x_f, x_i; k)$ at the poles $k = k_n$, which give the problem eigenenergies through $E_n = \hbar^2 k_n^2/(2m)$.

• By inspecting the above Green's functions, we see that they can diverge (consequently presenting poles) only if $g(k = k_n) = 0$, with

$$g(k) = 1 - r_O^{(1)}(k)\, r_A^{(1)}(k) \exp[2ik\ell_1].$$

• As an example, consider the vertex O being a generalized δ interaction of strength γ.

• The reflection and transmission coefficients for O are ($\hbar = m = 1$ and $N = 3$ edges)

$$\begin{aligned} r_O^{(1)}(k) &= r_O^{(i)}(k) = r_O^{(f)}(k) = r_O(k) \\ &= \frac{2\gamma - (N-2)ik}{Nik - 2\gamma} = \frac{2\gamma - ik}{3ik - 2\gamma}, \end{aligned}$$

$$\begin{aligned} t_O^{(1,i)}(k) &= t_O^{(f,1)}(k) = t_O^{(f,i)}(k) = t_O(k) \\ &= \frac{2ik}{Nik - 2\gamma} = \frac{2ik}{3ik - 2\gamma}. \end{aligned}$$

• For the vertex A we take the boundary condition $-\psi'(A) = \lambda\psi(A)$, leading to

$$r_A(k) = \frac{ik + \lambda}{ik - \lambda}.$$

• Any pole of the scattering amplitudes in the upper half of complex k-plane along the imaginary axis represents a bound energy.

• For example, for the usual (1D) Dirac δ-function with intensity $\gamma < 0$ (attractive δ), the transmission coefficient is $t_\delta = ik/(ik - \gamma)$. In this case, the unique negative energy reads $E_1 = k_1^2/2 = -\gamma^2/2$, where $k_1 = i|\gamma|$ is the only pole of $t_\delta(k)$.

• So, for our graph the eigenvalues are obtained from the following transcendental equation (with $\mathrm{Re}[k_n] = 0$ and $\mathrm{Im}[k_n] > 0$)

$$g(k_n) = 1 - \left(\frac{2\gamma - ik_n}{3ik_n - 2\gamma}\right)\left(\frac{ik_n + \lambda}{ik_n - \lambda}\right)\exp[i2k_n\ell_1] = 0.$$

• Further, we note that ($g'(k_n) \equiv dg(k)/dk|_{k=k_n}$)

$$\lim_{E\to E_n} \frac{(E - E_n)}{g(k)} = \frac{1}{2}\lim_{k\to k_n} \frac{(k^2 - k_n^2)}{g(k)} = \frac{k_n}{g'(k_n)}.$$

• So, the residue of G (x_i and x_f in the leads) is

$$\begin{aligned}\psi_n^{(f)}(x_f)\,\psi_n^{(i)*}(x_i) &= \frac{1}{2}\lim_{k\to k_n}(k^2-k_n^2)\,G_{fi}(x_f,x_i;k)\\ &= \Big\{\mathcal{N}_G(k_n)\,t_O(k_n)\,\exp[ik_nx_f]\Big\}\\ &\quad\times\Big\{\mathcal{N}_G(k_n)\,t_O(k_n)\,\exp[ik_nx_i]\Big\},\end{aligned}$$

• And that for G (x_i and x_f in edge 1) is

$$\begin{aligned}\psi_n^{(1)}(x_f)\,\psi_n^{(1)*}(x_i) &= \frac{1}{2}\lim_{k\to k_n}(k^2-k_n^2)\,G_{11}(x_f,x_i;k)\\ &= \Big\{\mathcal{N}_G(k_n)\Big(\exp[-ik_nx_f]\\ &\quad + r_O^{(1)}(k_n)\exp[ik_nx_f]\Big)\Big\}\\ &\quad\times\Big\{\mathcal{N}_G(k_n)\Big(\exp[-ik_nx_i]+\\ &\quad r_O^{(1)}(k_n)\exp[ik_nx_i]\Big)\Big\}.\end{aligned}$$

Here

$$\mathcal{N}_G(k_n) = \frac{1}{\sqrt{ig'(k_n)\,r_O^{(1)}(k_n)}}.$$

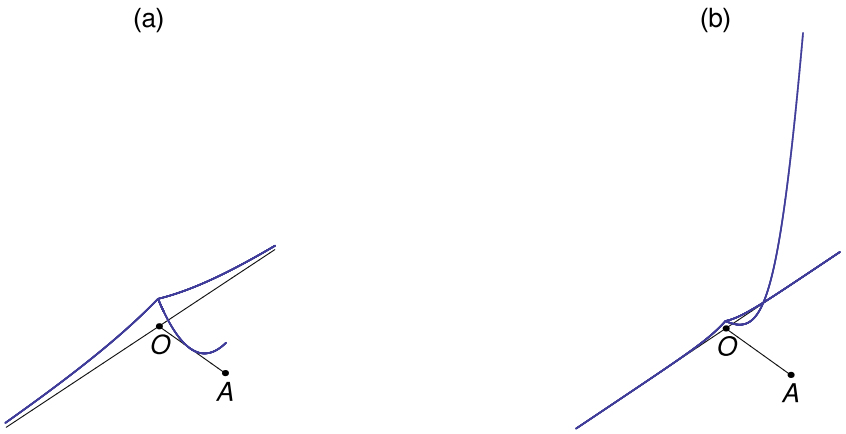

Figure 6: The bound eigenstates probability distribution along the quantum graph, $\ell_1 = 1$. The vertex O is a δ interaction of strength $\gamma = -3/2$. At A we have $-\psi'(A) = \lambda\psi(A)$, with $\lambda = -2$. (a) $|\psi_1(x)|^2$ for which $\kappa_1 = 0.463618$ and (b) $|\psi_2(x)|^2$ for which $\kappa_2 = 2.022448$.

• For $k_n = i\kappa_n$, with $\kappa_n > 0$, ψ in both leads have the general form $\psi_n(x) = \mathcal{N} \exp[-\kappa_n x]$ $(x \geq 0)$. Hence, they decay away from the origin (vertex O) exponentially, as it should be. The $\mathcal{N}$'s also lead to the correct normalization for the eigenstates. The same results follow from the direct solution of the Schrödinger equation

• For our G with the end points in the leads i and f, as already discussed, the quantity $|T_{fi}|^2$ (in G_{fi}) can be interpreted as the total probability for a particle of wave number k incident from the lead i to be transmitted to the lead f.

• Similarly, for x_i and x_f in lead i, we have

$$G_{ii}(x_f, x_i; k) = \frac{m}{i\hbar^2 k}\Big\{ \exp[ik|x_f - x_i|] + R_i \exp[ik(x_f + x_i)]\Big\},$$

$$R_i = r_O^{(i)} + \frac{t_O^{(1,i)}\, r_A^{(1)}\, t_O^{(i,1)} \exp[2ik\ell_1]}{1 - r_O^{(1)}\, r_A^{(1)} \exp[2ik\ell_1]}.$$

• Then, $|R_i|^2$ represents the total probability for a particle of wave number k incident from the lead i to be reflected to the lead i. By choosing different quantum amplitudes for the vertices, we naturally get different scattering patterns from R_i and T_{fi}.

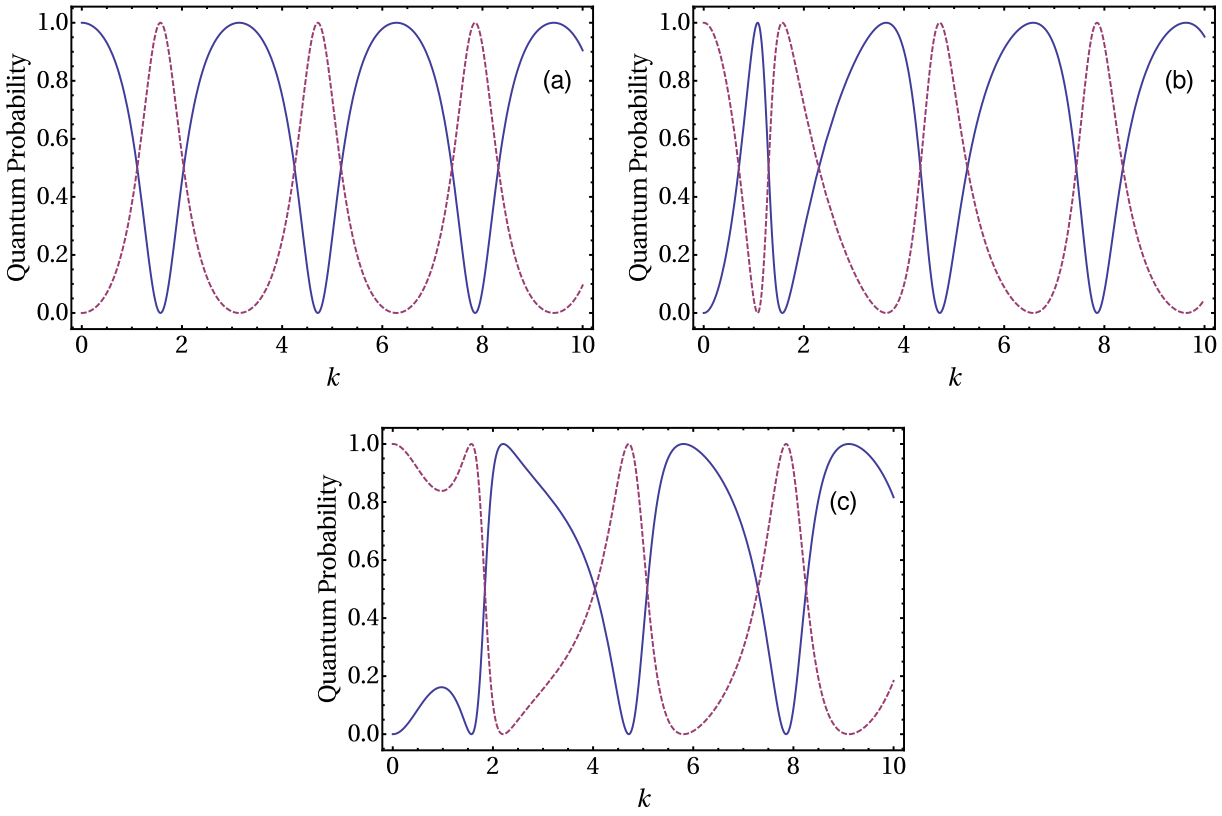

Figure 7: Transmission $|T_{fi}|^2$ (solid) and reflection $|R_i|^2$ (dashed) probabilities versus $= k$ for $\lambda = 0$ (Neumann-Kirchhoff bc at A). γ at O: (a) 0, (b) 1, and (c) -3/2.

• Let us assume the Neumann-Kirchhoff boundary conditions at the vertex A, so we set $\lambda = 0$ in r for A (with $\ell_1 = 1$). For O, we consider three values for the parameter γ: (a) $\gamma = 0$ (so, also Neumann-Kirchhoff); and the generalized δ of strengths (b) $\gamma = 1$ and (c) $\gamma = -3/2$.

REPRESENTATIVE QUANTUM GRAPHS

- The widely analyzed (with the most distinct purposes, like to investigate scattering features of 3D graphs) hypercube;

- The binary tree, e.g., useful to highlight differences between classical and quantum walks as well as to test the speed up gain – which is actually exponential – in searching algorithms based on quantum dynamics. We should observe that the graph of Fig. 4 (a) is in fact an extension of a binary tree, being a fragment of a large-scale ternary tree network;

- Triangular Sierpiński-like structures, a nice illustration of graphs which in the limit of infinite vertices would be fractal. It has been considered in connection with molecular assembling and with the mathematics of logical games like the Hanoi tower.

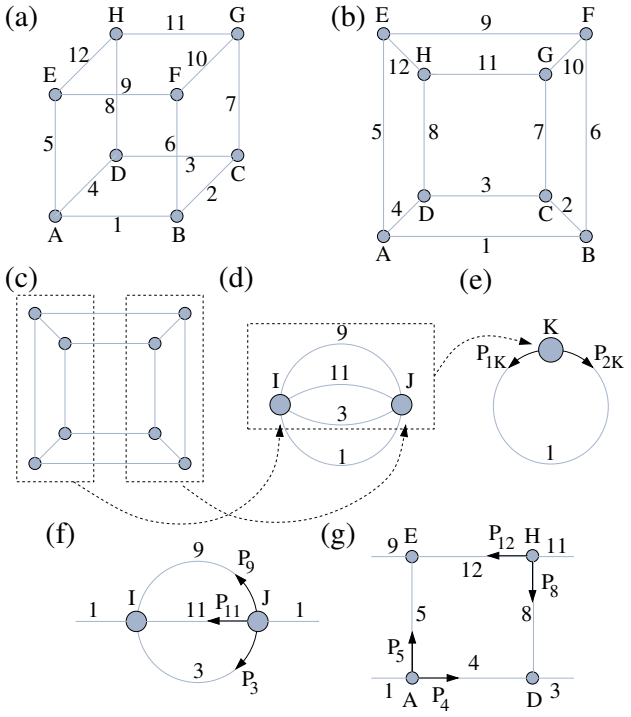

Figure 8: A cube quantum graph. (a) The letters represent the vertices indices and the integers the edges indices. (b) A cube graph planar representation. (c)-(e) Regrouping procedures (see the main text). (f) Auxiliary graph to determine the total R's and T's. (g) The inner structure of vertex I. The P_l's indicate the sp families.

• The Green's function for closed graphs can be obtained by the regrouping technique. Thus, once can use this procedure to get the Green's function for the cube quantum graph of Fig. 8 (a) (where all edges have length ℓ). In Fig. 8 (b) we show a planar representation of the cube.

• Now, let us examine the closed cube graph eigenstates supposing all the vertices having the same properties. Hence, for the cube eight vertices we assume the generalized δ interaction.

• The eigenenergies come from the poles of G, i.e., from the roots of: $g = (1 - T(k)\exp[ik\ell])^2 - R(k)^2\exp[2ik\ell] = 0$. Note this is a very symmetric case, so all T's and R's are equal.

In the Table we show the resulting first ten eigenvalues for $\gamma = 0$ and $\gamma = 1$ ($m = \hbar = 1$).

	γ	
State	0	1
1	1.230959	1.094322
2	1.919633	1.642395
3	3.141593	2.190764
4	4.372552	3.141593
5	5.052226	3.516328
6	6.283185	5.177393
7	7.514145	6.283185
8	8.193819	7.602957
9	9.424778	8.273085
10	10.65574	9.424778

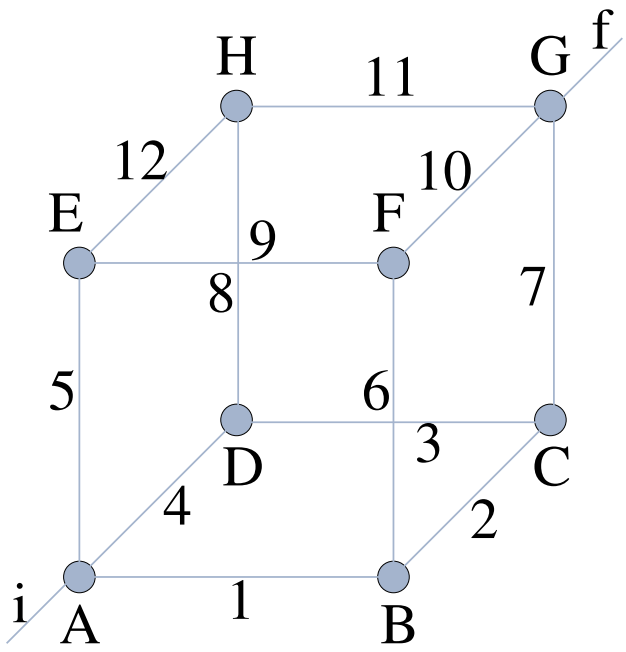

Figure 9: The original quantum closed cube graph is attached to two leads (at the vertices A and G), thus becoming an open graph structure.

• One also can study scattering through the original closed cube by attaching leads to it. In Fig. 9 we display a possible configuration, where leads are added to the vertices A and G of our previous very symmetric graph. For the now modified vertices A and G, we also assume a δ interaction of strength γ, only recalling that in this case these two vertices have a coordination number $N = 4$ (instead of $N = 3$).

• Calculating T_{fi} (and also R_i) using the discussed techniques, we show in Fig. 10 the transmission and reflection probabilities as function of k for $\gamma = 0$ and $\gamma = 1$. Since for the former the individual edges transmission and reflections coefficients are not function of k, we do not see $|T_{fi}|^2$ tending to 1 for k increasing (as slowly seen for $\gamma = 1$).

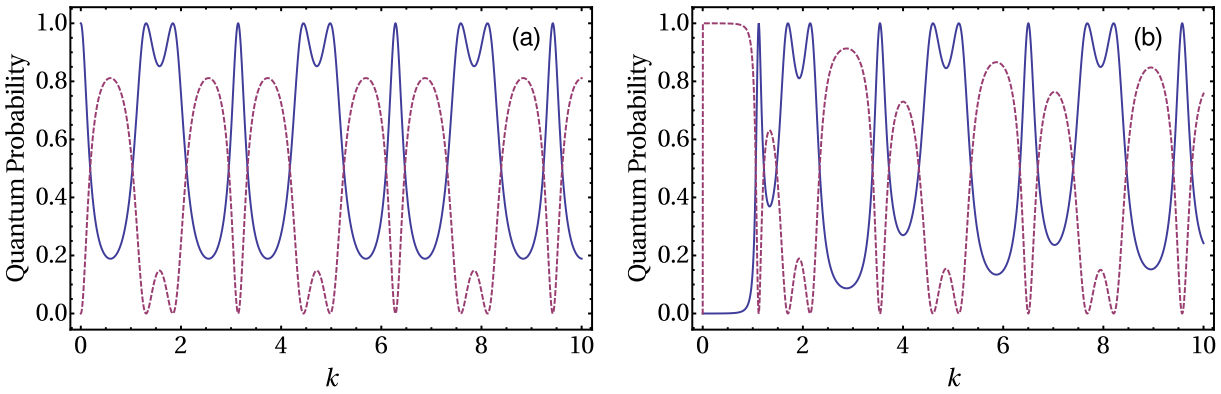

Figure 10: The transmission $|T_{fi}|^2$ (solid line) and reflection $|R_i|^2$ (dashed) probabilities for the open cube graph of Fig. 9. All the vertices are generalized δ interactions of strength (a) $\gamma = 0$ and (b) $\gamma = 1$. Here $m = \hbar = 1$.

• As previously emphasized, the general way the Green's function can be written in terms of arbitrary quantum coefficients – encompassing 'blocks' of vertices and edges – allows one to use a recursive procedure to obtain the system full solution. This is a particularly useful protocol for graphs displaying a hierarchical structure, as the case of the binary tree depicted in Fig. 11 (which illustrates three 'levels' ($l = 1, 2, 3$) of the graph construction by insertions). In the following we assume all the edges having the same length ℓ (so, Fig. 11 is not shown in scale).

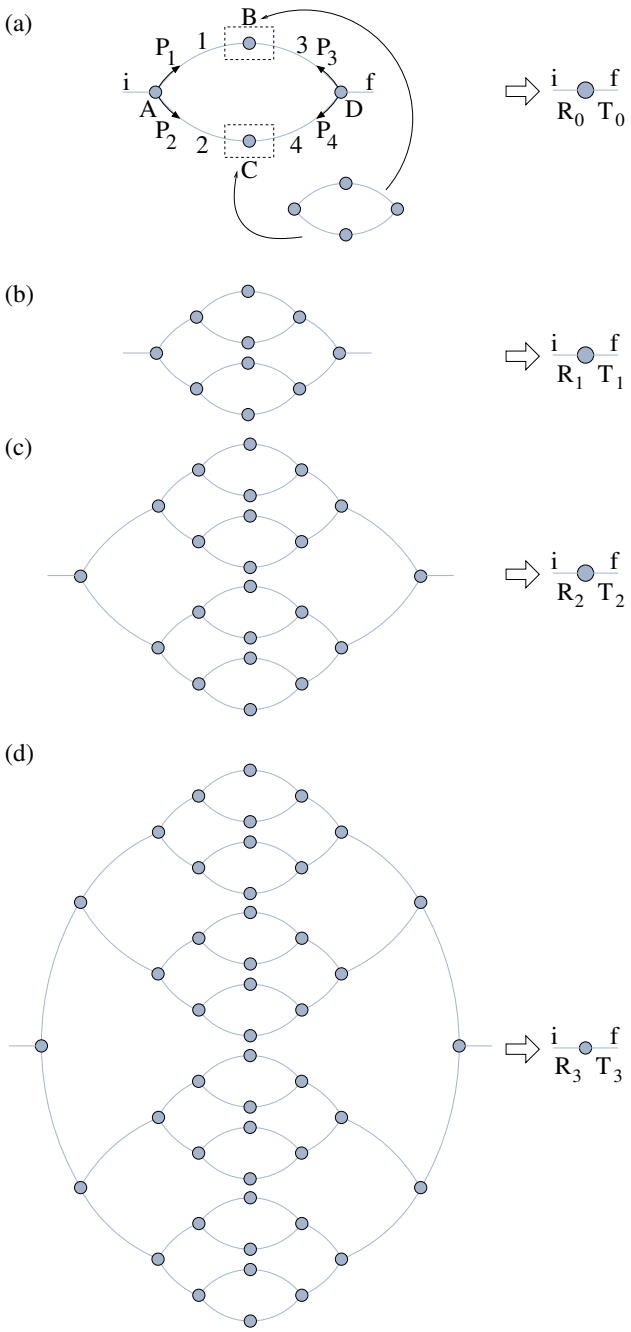

Figure 11: Binary tree (attached to leads i and f) with different number of recursive compositions l.

• As a numerical example, consider the edges with the same length $\ell = 1$ and Dirac δ interactions of intensity γ (for $\gamma = 0$ and $\gamma = 1$) as the boundary conditions at all the vertices. For the vertices with $N = 2$ edges (say B and C) we have $r = \gamma/(ik - \gamma)$ and $t = ik/(ik - 2\gamma)$ and for those with $N = 3$ (say A and D) $r = (2\gamma - ik)/(3ik - 2\gamma)$ and $t = 2ik/(3ik - 2\gamma)$. In the figure we show the reflection $|R_l|^2$ ($i \to i$) and transmission $|T_l|^2$ ($i \to f$) probabilities for the basic structure (Fig. 11 (a)) and for the three levels of insertions for the binary tree (Fig. 11 (b)–(d)). As it should be expected, for higher l's the patterns of reflection and transmission, as function of k, become much more complex. Also, we do not observe any systematic increasing of $|T_l|^2$ as k increases because the rich interference behavior – due to the wave propagation along the distinct edges – takes place for any value of k.

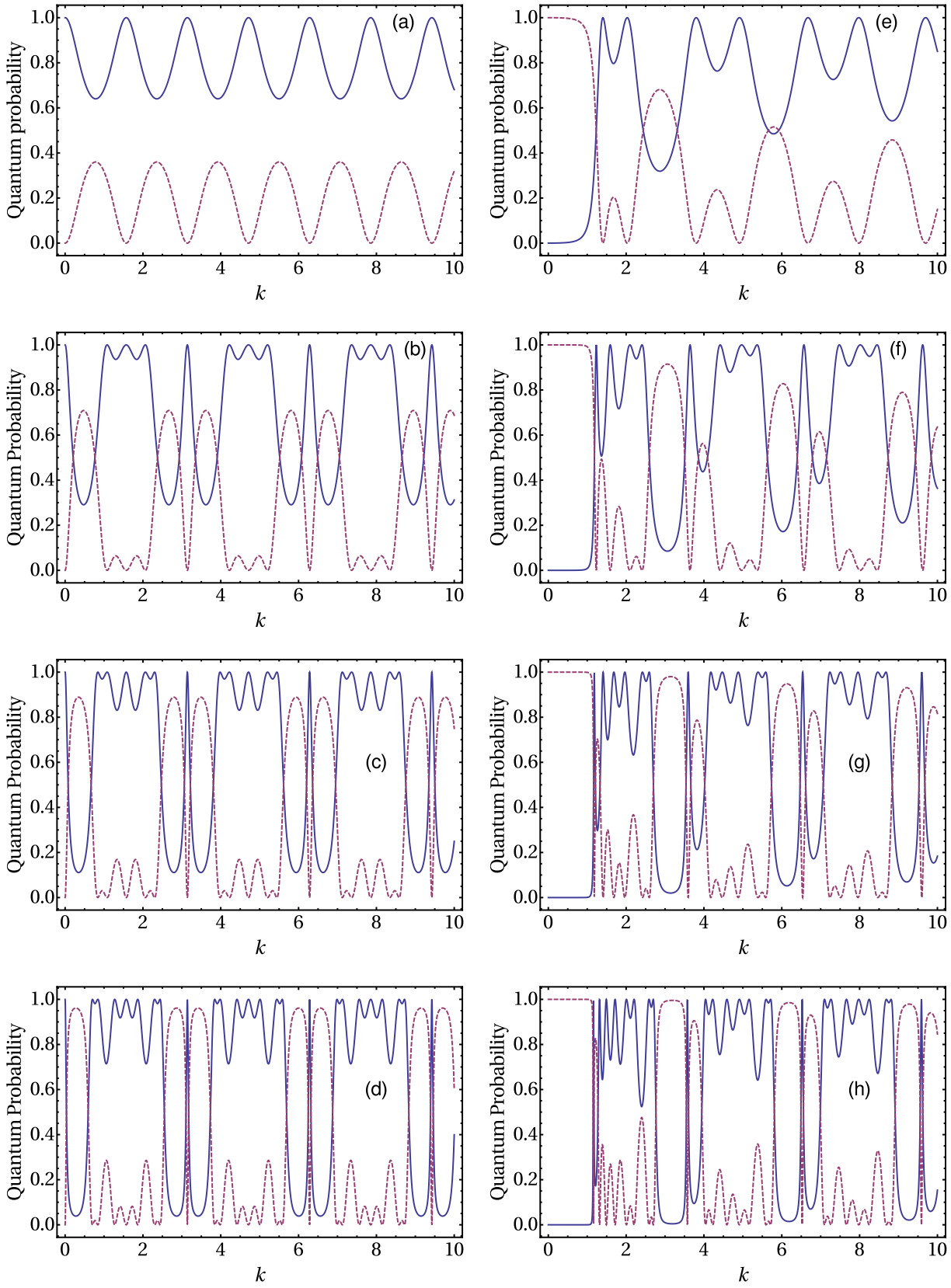

Figure 12: The transmission $|T_l|^2$ (solid line) and reflection $|R_l|^2$ (dashed) probabilities for the binary trees of Fig. 11.

• One of the many reasons for the interest in self-similar lattices is their utility to model systems which are self-assembled from an original backbone (the motif of the replication), the case of certain complex molecules. Sierpiński graphs are very nice examples of structures which can be recursively generated from a basic building block. They originate from the Sierpiński gasket, a well-known fractal object introduced by Sierpiński in 1915.

• Sierpiński graphs have been studied in relation to small-world networks Also, Sierpiński gaskets have been analyzed elsewhere, where Neumann-Kirchhoff boundary conditions were considered. However, the most general case of arbitrary reflection and transmission amplitudes for the vertices are still not well explored in the literature.

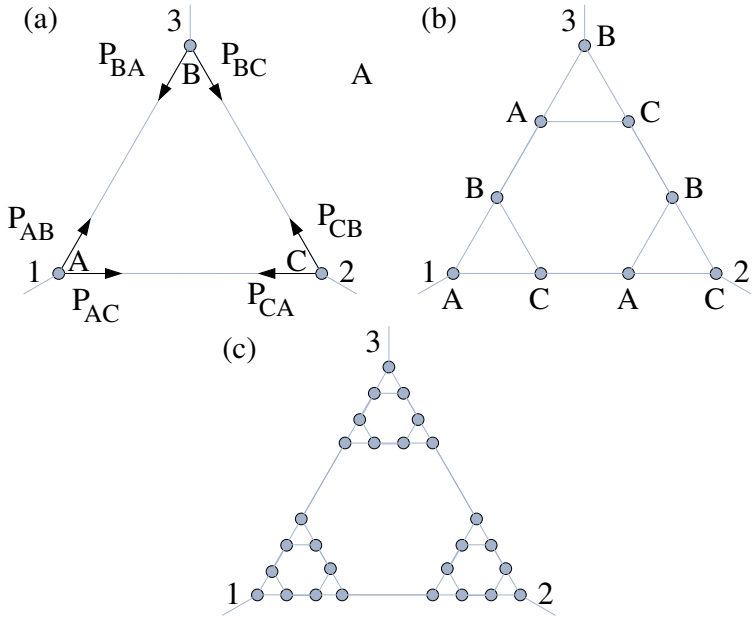

Figure 13: Finite Sierpiński graphs with different number n of recursive stages: (a) $n = 1$ (the initial Δ_{ABC} structure), (b) $n = 2$, and (c) $n = 3$. The P's in (a) represent proper infinite families of scattering paths useful to calculate G. The generation of new vertices from (a) to (b) illustrates the elementary transformation to Δ_{ABC}, the basic step leading to the successive graph stages.

• In Fig. 13 we show three different stages ($n = 1, 2, 3$) of a Sierpiński graph. The basic step to go from n to $n + 1$ involves a transformation in all the fundamental equilateral triangles Δ_{ABC} of the graph n.

• Since at any stage n the graph always has exactly three semi-infinite leads, the scattering matrix is of order 3 and given by

$$S_n = \begin{pmatrix} R_n^{(1)} & T_n^{(1,2)} & T_n^{(1,3)} \\ T_n^{(2,1)} & R_n^{(2)} & T_n^{(2,3)} \\ T_n^{(3,1)} & T_n^{(3,2)} & R_n^{(3)} \end{pmatrix}.$$

• Above, $R_n^{(a)}$ and $T_n^{(b,a)}$ are the resulting reflection (from lead a $(= 1, 2, 3)$) and transmission (from lead a to lead b, with $a \neq b$ and $a, b = 1, 2, 3$) amplitudes for the group of 3^n vertices constituting the Sierpiński graph at stage n (see Fig. 13).

• Setting $\ell = \ell_1 = 1$ and the same delta point interaction of strength γ at all the elementary vertices A, B, and C, we show in Fig. 14 ($\gamma = 0$) and Fig. 15 ($\gamma = 1$), the behavior of the reflection and transmission coefficients as function of k for the Sierpiński graph stage n, up to $n = 5$. We notice that as n increases, the system becomes more and more selective to which k's (or equivalently, energies) can be transmitted through the structure. This effect is stronger for $\gamma = 1$ (Fig. 15) since then the elementary r's and t's are also k-dependent. So, in this respect the Sierpiński graph at the different stages contrasts with the binary tree at different levels, for which there is not a such filter-like phenomenon.

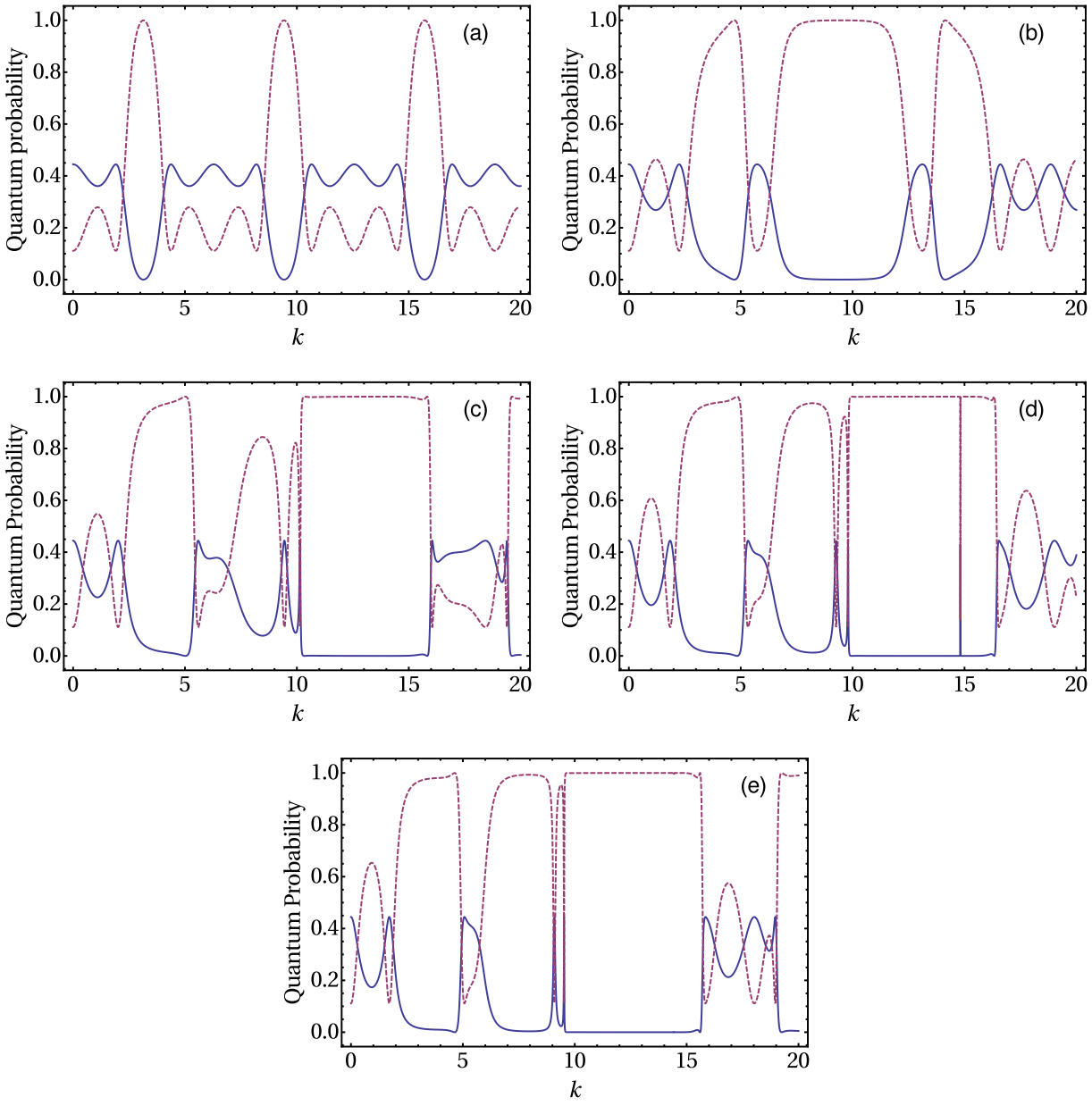

Figure 14: The transmission $|T_n|^2$ (solid line) and reflection $|R_n|^2$ (dashed) probabilities for the stage n of the Sierpiński graph, Fig. 13. Here $\ell = \ell_1 = 1$ and at any elementary vertex A, B, and C, we assume a same generalized δ interaction of strength $\gamma = 0$. The cases $n = 1$, $n = 2$, $n = 3$, $n = 4$, and $n = 5$, are displayed, respectively, in (a), (b), (c), (d) and (e).

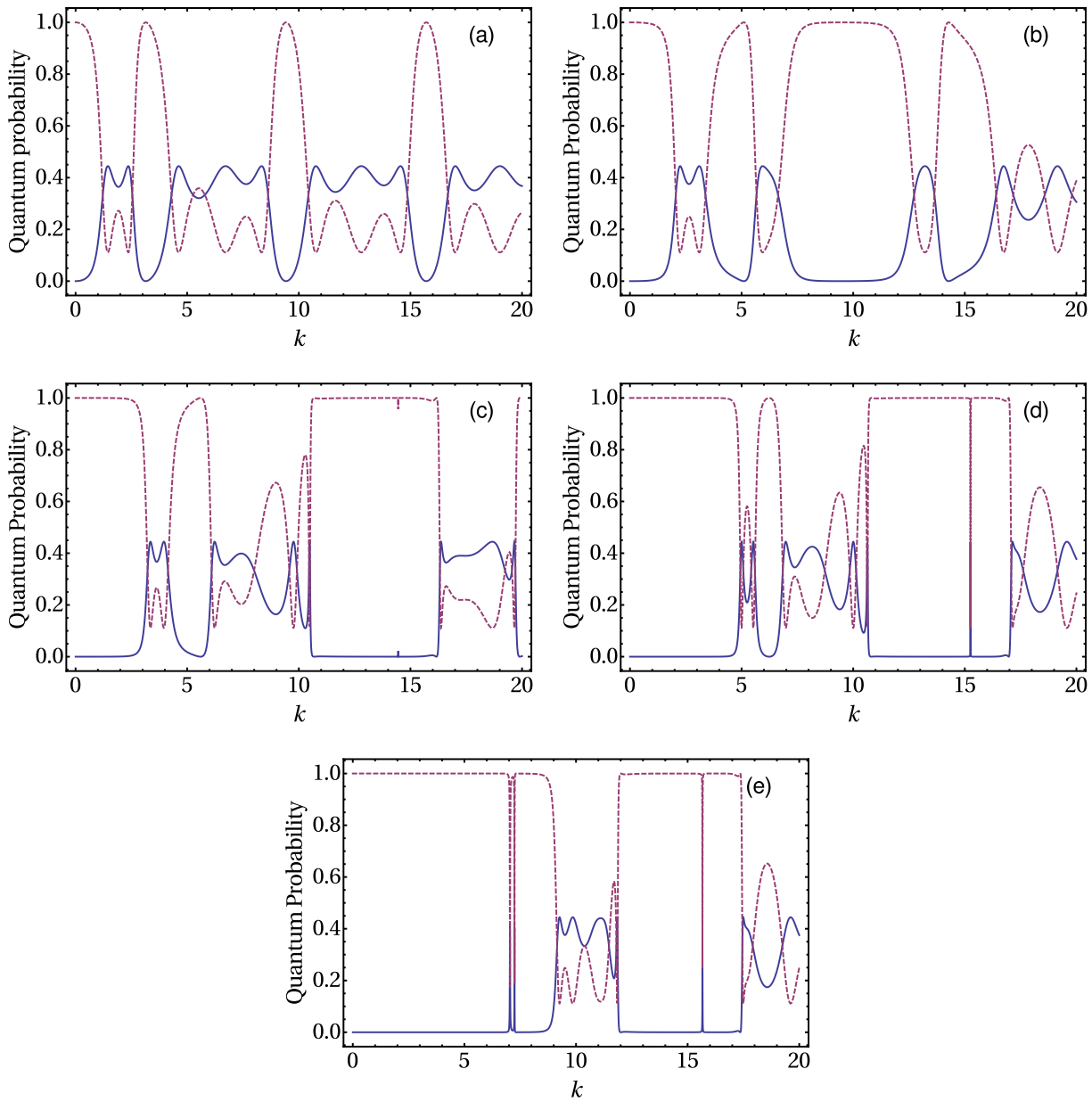

Figure 15: The same as in Fig. 14, but for $\gamma = 1$.

PROBING THE TRANSMISSION FLUX IN PARTS OF A QUANTUM GRAPH

• Let us recall that $G(x_f, x_i; k)$ can be generally interpreted as the transition probability amplitude for a particle (of energy E) initially in x_i (lead i) to get to x_f in edge e_l. Thus, the overall multiplicative term for $\exp[iS(x_f, x_i; k)/\hbar]$ in the formula for G typically will be

$$\mathcal{A}_{i,l} = \frac{T_{i,l}}{1 - R_{\text{right}} R_{\text{left}} \exp[2ik\ell_l]}.$$

• So, if the graph supports a quasi-bound state totally or partially localized in e_l, an incident wave (from lead i) with k close to the corresponding quasi-bound state $k^{(\text{qb})}$ value should have a very high probability to be transmitted to the edge e_l region and $|\mathcal{A}_{i,l}|^2$ would be high.

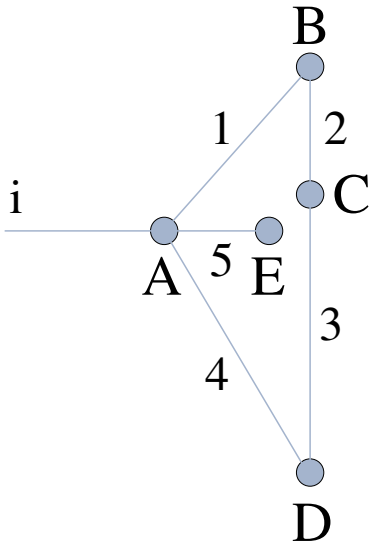

Figure 16: An open graph, whose a modified version has been studied in [J. Phys. A **36**, L545 (2003)] in the context of quantum protocols for information transmission.

• On the other hand, if for the scattering process, the system geometry is such that destructive interference makes ψ in e_l to be very low, then this also should be the case for $|\mathcal{A}_{i,l}|^2$.

• Consider the structure in Fig 16. Such graph can display interesting features if one assumes different boundary conditions at each vertex and distinct lengths for each edge.

• We consider generalized delta interactions of a same γ at A, B, C, D, and either Dirichlet or Neumann boundary conditions at E. Also, we suppose all the edges with the length $\ell = 1$. Due to symmetry, the edges 1 and 4 and 2 and 3 must present similar scattering properties and we can focus just on the inequivalent amplitudes $\mathcal{A}_{i,1}(k)$, $\mathcal{A}_{i,2}(k)$, and $\mathcal{A}_{i,5}(k)$.

• We show in Fig. 17 the behavior of the modulus square of these three quantities as function of k for the Dirichlet and Neumann boundary conditions at E and the delta interactions strength value $\gamma = 0.5$ and $\gamma = 1$.

• We observe a richer profile of resonances. Also, the distinct boundary conditions at E considerably change the positions and sizes of the $E^{(\mathrm{qb})}$ peaks. In general the peaks are higher and narrower, so longer-lived, for the greater value of γ ($\gamma = 1$).

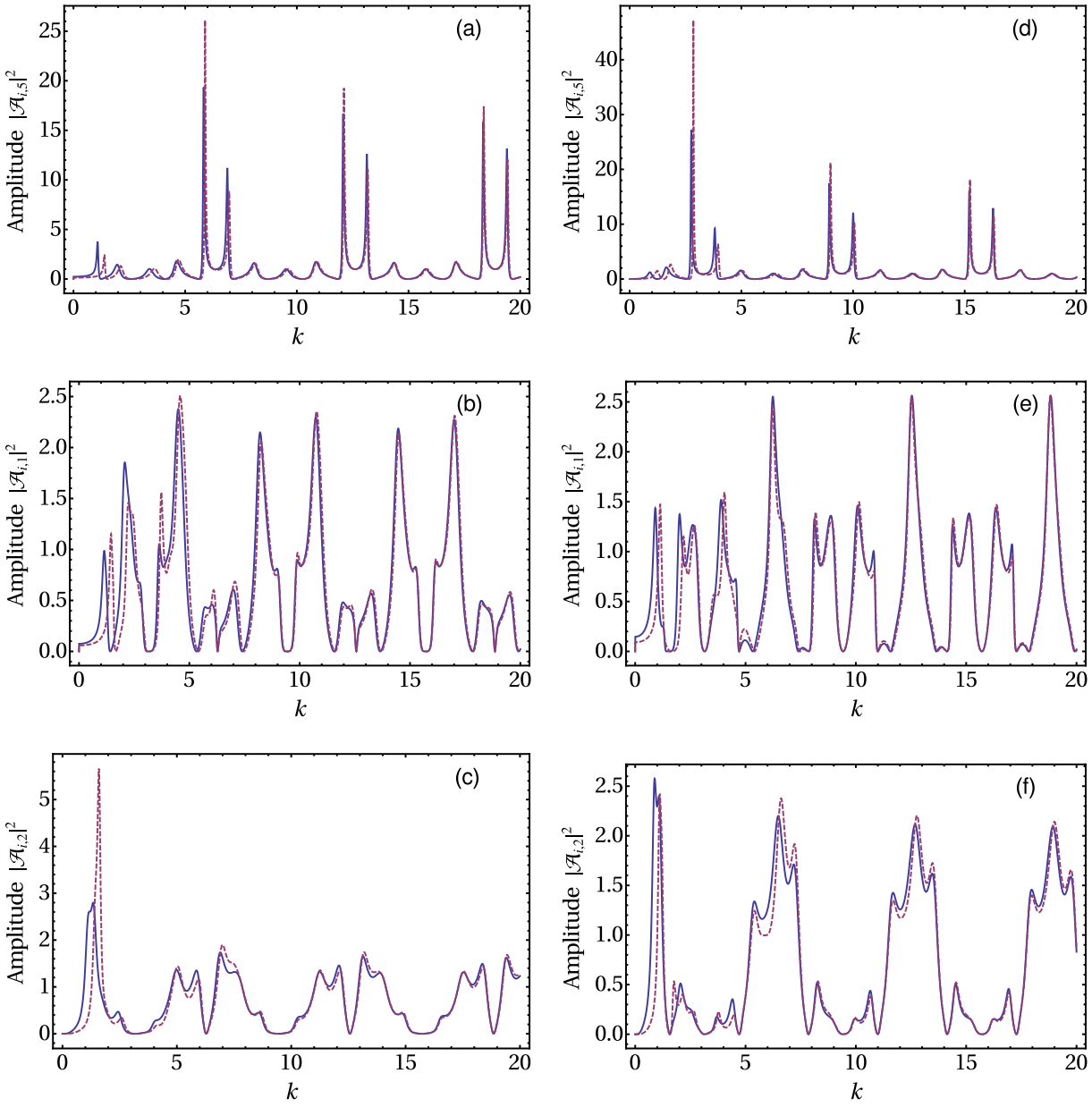

Figure 17: Behavior of $|\mathcal{A}_{i,l}|^2$ as function of k for $l = 1, 2, 5$. The vertices A, B, C, and D, are generalized delta interactions of strength γ, with $\gamma = 0.5$ (solid) and $\gamma = 1$ (dashed) lines. The boundary conditions at vertex E are Dirichlet's (so, $r_E = -1$) in (a)–(c) and Neumann's (so, $r_E = 1$) in (d)–(f). All edges have the same length $\ell = 1$.

Conclusion (few take home messages)

- Interesting systems still can be treated exactly through path integrals approach
- Graph structures are amazing systems to test different fundamental and applied aspects of quantum mechanics
- Semiclassical and semiclassical-like approximations are still very useful tools to treat quantum systems in the realm of path integrals
- Similar systems to quantum graphs, notably, quantum walks can be treated using the same ideas here

Many thanks Ubu!